Journal of Nuclear Medicine, published on August 6, 2020 as doi:10.2967/jnumed.120.248120

Urokinase Plasminogen Activator Receptor (uPAR) PET/MRI of Prostate Cancer for Non-invasive Evaluation of Aggressiveness: a Prospective Phase II Clinical Trial Comparing with Gleason Score

Marie Øbro Fosbøl[1], Sorel Kurbegovic[1], Helle Hjorth Johannesen[1], Martin Andreas Røder[2], Adam Espe Hansen[1], Jann Mortensen[1], Annika Loft[1], Peter Meidahl Petersen[3], Jacob Madsen[1], Klaus Brasso[2], Andreas Kjaer[1,*]

[1]Department of Clinical Physiology, Nuclear Medicine & PET and Cluster for Molecular Imaging, Rigshospitalet and University of Copenhagen, Denmark

[2] Copenhagen Prostate Cancer Center, Department of Urology, Rigshospitalet, Copenhagen, Denmark

[3] Department of clinical oncology, Rigshospitalet, Copenhagen, Denmark

***) Corresponding author**: Prof. Andreas Kjaer, E-mail: akjaer@sund.ku.dk

Address: Department of Clinical Physiology, Nuclear Medicine & PET. Rigshospitalet, Blegdamsvej 9, DK 2100 Copenhagen, Denmark

First author: PhD student Marie Øbro Fosbøl, E-mail: marie.oebro.fosboel@regionh.dk

Address: Department of Clinical Physiology, Nuclear Medicine & PET. Rigshospitalet, Blegdamsvej 9, DK 2100 Copenhagen, Denmark

Word count: 4.703

Running title: uPAR-PET in prostate cancer

Key words: urokinase-type plasminogen activator receptor (uPAR), prostate cancer, PET, PET/MRI, risk stratification, active surveillance, Gleason score

ABSTRACT

The **aim** of this study was to evaluate the correlation between uptake of the positron emission tomography (PET) ligand ^{68}Ga-NOTA-AE105 targeting the urokinase-type plasminogen activator receptor (uPAR) and Gleason score in patients undergoing prostate biopsy. **Materials & methods:** Patients with clinical suspicion of prostate cancer (PCa) or previously diagnosed with PCa were prospectively enrolled in this phase II trial. A combined uPAR PET, multiparametric magnetic resonance imaging (mpMRI) was performed and standardized uptake value (SUV) from primary tumor, as delineated by mpMRI, was measured by two independent readers. Correlation between SUV and Gleason score obtained by biopsy was assessed. **Results:** A total of 27 patients had histologically verified PCa visible on mpMRI and constituted the study population. There was a positive correlation between SUV_{max} and Gleason score (Spearman's rho= 0.55; p=0.003). Receiver operating characteristics analysis showed an area under the curve (AUC) of 0.88 (95%CI: 0.67-1.00) in discriminating Gleason score ≥3+4 from ≤3+3. A cut-off for tumor SUVmax could be established with a sensitivity of 96% (79-99%) and specificity of 75% (30-95%) in detecting Gleason Scores ≥3+4. For discriminating Gleason score ≥ 4+3 vs. ≤ 3+4, a cut-off could be established for detecting Gleason score ≥ 4+3 with a sensitivity of 93% (69-99%) and specificity of 62% (36-82%). **Conclusion:** SUV measurements from uPAR PET in primary tumors as delineated by mpMRI showed a significant correlation with Gleason score, and tumor SUV_{max} was able to discriminate between low-risk and intermediate risk Gleason score profiles with high diagnostic accuracy. Consequently, uPAR PET/MRI could be a promising method for non-invasive evaluation of PCa, which may in the future potentially reduce the need for repeated biopsies, e.g. in active surveillance.

INTRODUCTION

Prostate cancer (PCa) is highly variable in nature ranging from a low-risk disease, which can be monitored by active surveillance, to a more aggressive disease, which requires prompt definitive treatment. Accurate methods for risk assessment are important in order to reduce the number of unnecessary interventions in patients with low-risk disease, but also to avoid delays in potential curative therapy (*1*–*3*). Current stratification is based on serum prostate specific antigen (PSA), clinical tumor stage, and histopathological grading by Gleason score (GS) in biopsy material. Recently, multiparametric magnetic resonance imaging (mpMRI) has also been incorporated in prostate cancer guidelines for detection and as a tool for targeting biopsies (*4*,*5*). Using mpMRI for targeting biopsies increase the number of clinically significant cancers detected, which is an important advancement in the management of PCa (*5*–*7*).

During active surveillance, repeated biopsies to detect histopathological progression are a key element. However, repeated biopsies may show results different from the primary biopsy as a consequence of sampling error. To circumvent sampling error and to replace an invasive method with a non-invasive method, molecular imaging targeting markers of aggressiveness, e.g. with positron emission tomography (PET), could be an ideal method. The risk of sampling error in tissue biopsies is overcome, as the entire tumor volume is assessed by imaging. In this context, combining PET and mpMRI is an appealing option where mpMRI serves the goal of achieving a reproducible delineation of the tumor to guide the PET readout.

Urokinase-type plasminogen activator receptor (uPAR) is a cell membrane protein involved in extracellular matrix degradation. In addition to regulating proteolysis, uPAR activates many intracellular signaling pathways that promote invasion, and proliferation through cooperation with transmembrane receptors. uPAR is frequently overexpressed in malignant tissue and high expression levels are associated with cancer invasion, metastatic potential and resistance to chemotherapy (*8*–*12*). In clinical studies of prostatectomy specimens uPAR expression levels in tumor tissue are associated with higher pathological tumor stage, higher GS, positive surgical margins and shorter biochemical recurrence free survival (*13*,*14*). These observations support that non-invasive evaluation of uPAR expression could become a clinically relevant prognostic imaging biomarker, with the possibility of distinguishing indolent tumors from the invasive phenotype, which subsequently could be used as a non-invasive replacement of biopsies during active surveillance.

For uPAR-PET, several radioligands based on the high affinity peptide antagonist AE105 have been developed (*15*–*19*). Phase I studies have been published both with ^{68}Ga-NOTA-AE105 and ^{64}Cu-DOTA-AE105 in patients with various cancer types – including PCa (*20*,*21*). Both ligands accumulated in primary tumor lesions as well as metastases and the uptake corresponded with high uPAR expression in excised tumor tissue, thereby providing evidence for uPAR PET imaging being target specific.

The aim of this exploratory phase II study was to investigate the use of ^{68}Ga-NOTA-AE105 uPAR-PET as a tool for evaluation of localized PCa. Accordingly, the predefined, primary outcome measure was to study the correlation between uPAR ligand uptake in the primary tumor and GS obtained from biopsy material.

METHODS

Study design

Between Nov. 2017 and Sept. 2019, we included 52 men fulfilling one of the two criteria; either suspicion of PCa based on clinical findings or previously diagnosed PCa prior to re-biopsies in an active surveillance program. Included patients underwent uPAR-PET/mpMRI before initiation of any anti-tumor therapy. Exclusion criteria were obesity (body weight > 140 kg due to scanner safety limits), severe claustrophobia or metallic foreign bodies not compatible with MRI. Eligible patients were included after giving informed consent.

The PCa diagnosis was verified histologically following transrectal MRI-directed cognitive-fusion guided biopsy. GS and localization of lesions from the pathology report served as reference for the study outcome.

The study protocol was approved by the Danish Health and Medicine Authority (EudraCT no. 2017-002276-37) and the Ethical Committee of the Capital Region of Denmark (protocol no. H-17019311). Signature of written informed consent was obtained from all patients. The study was registered in ClinicalTrials.gov (NCT03307460) and was performed in accordance with the recommendation for Good Clinical Practice (GCP) including independent monitoring by the GCP unit of the Capital Region of Denmark.

PET/mpMRI acquisition

^{68}Ga-NOTA-AE105 PET and mpMRI was performed simultaneously using an integrated whole-body PET/MRI system (Siemens Biograph mMR, Siemens Healthcare, Erlangen, Germany). PET was performed as a 45 minutes scan starting at injection of approximately 200 MBq ^{68}Ga-NOTA-AE105. Synthesis of the ligand was performed as previously described (*21*). Patients were asked to void before the examination, no bladder catheter or rectal coil was applied. Patients had crossed arms over the chest, and arms did not enter the FOV at the level of prostate.

PET was reconstructed using vendor-provided Dixon-based MR attenuation correction (MRAC) with an atlas-based bone segmentation, and with absolute scatter correction (3D OP-OSEM, 3 iterations, 21 subsets, 4 mm Gaussian filter). Images used for interpretation and quantification were reconstruction of data acquired 20-30 minutes post injection.

mpMRI protocol

3 T MRI included: Transverse T1-weighted Turbo Spin Echo (TSE) [TE 20 ms, TR 735 ms, pixel size: 0.7×0.7 mm^2, slice thickness 5.0 mm]; vendor provided Dixon-VIBE (volumetric interpolated breath-hold examination) for PET attenuation correction [voxel size: 1.3×1.3×3.0 mm^3]; sagittal T2-weighted TSE [TE 101 ms, TR 5,590 ms, pixel size: 0.6×0.6 mm^2, slice thickness 3.0 mm]; coronal T2 TSE [TE 101 ms, TR 6,050 ms, pixel size: 0.6×0.6 mm^2, slice thickness 3.0 mm]; transverse T2 TSE [TE 104 ms, TR 7,480 ms, pixel size: 0.5×0.5 mm^2, slice thickness 3.0 mm]; Diffusion Weighted (DW) single-shot spin-echo echo-planar imaging [TE 60 ms, TR 5,700 ms, pixel size: 2.0×2.0 mm^2, slice

thickness 3.0 mm, b-values: 0, 800 s/mm^2] and [TE 66 ms, TR 5,700 ms, pixel size: 2.0×2.0 mm^2, slice thickness 3.0 mm, b-value: 1400 s/mm^2]; Dynamic Contrast-Enhanced (DCE) VIBE [TE 1.78 ms, TR 5.18 ms, pixel size: 1.4×1.4×3.6 mm^3, 35 repetitions, acquisition time 4 minutes 25 seconds, bolus of Gadovist contrast agent (0.1 ml/kg, 1 mmol/ml) administered after 2nd repetition].

Image analysis

All image data was analyzed by two certified specialists in nuclear medicine and an experienced certified specialist in MRI radiology. mpMRI was interpreted according to Prostate Imaging Reporting and Data System 2.0 (PI-RADS) (*22*) and reviewed by the radiologist and treating urologist together before mpMRI-directed cognitive-fusion guided biopsy was performed.

Blinded to PET results, volumes of interest (VOIs) corresponding to lesions identified on mpMRI, were drawn on T2 weighted MR images using Mirada DBx (Mirada Medical, Oxford, UK). Where necessary, the VOIs were subsequently adjusted by the nuclear medicine specialists to avoid inclusion of signal from the urinary bladder. Uptake of the uPAR ligand in the MRI VOIs was parameterized as maximum standardized uptake value (SUV_{max}).

Statistical analysis

Patient characteristics were reported by descriptive statistics including age, PSA, clinical tumor (cT) stage, and pathological tumor (pT) stage (when available). In case of multiple lesions per

patient, the lesion with the highest SUV_{max} was included in the analysis. Spearman rank correlation was used to estimate correlation between SUV and pathological features measured on an ordinal scale. Inter reader reliability of SUV-measurement was estimated using intraclass correlation coefficient (ICC). Comparison of distribution of continuous data was performed with independent samples T test. Determination of optimal cut-off in discrimination between GS 3+3 vs. ≥ GS 3+4 and GS ≤ 3+4 vs. ≥ 4+3 was performed with an R-package developed by Budczies et al. (*23*).

A p-value of < 0.05 was considered statistically significant. Statistical analyses were performed using IBM SPSS Statistics v. 22 (IBM Corp. Armonk, NY) and R (http://www.R-project.org).

RESULTS

A total of 52 patients were enrolled in the study. Due to exclusions and technical issues, 46 patients had both PET/MRI and histology available. Of these, 16 patients had no suspicious lesions on mpMRI and further three patients had negative histology leaving a study population of 27 patients for analysis (Figure 1). Of these, six patients were enrolled prior to re-biopsies in an active surveillance program, while the remaining 21 patients were enrolled as they were scheduled to undergo biopsies based on clinical suspicion of PCa. Patient characteristics are shown in Table 1.

Patients received an intravenous dose of approximately 200 MBq (median 211 MBq, range: 154-234 MBq) ^{68}Ga-NOTA-AE105, which according to dosimetry calculations from the phase I trial corresponds to an effective dose of approximately 3.1 mSv (*21*). None of the patients experienced reactions or adverse events related to the administration.

Interobserver reliability in measurement of tumor SUV_{max} was excellent with an ICC of 0.90 (95% CI: 0.79-0.95). There was a significant positive correlation between tumor VOI SUV_{max} and GS from biopsy material with a correlation coefficient of 0.55 (p=0.003) (Figure 2). Mean SUV_{max} based on GS is displayed in table 2.

To estimate the ability of SUV_{max} for discrimination between GS groups, receiver operating characteristic analyses were performed. For discrimination between GS ≤ 3+3 vs. GS ≥3+4 area under the curve (AUC) for SUV_{max} was 0.88 (95% CI: 0.67-1.00, p=0.017). Optimal cutoff for achieving >90% sensitivity for detecting GS ≥3+4 was SUV_{max} = 2.75 (Figure 3). The suggested cut-off showed a sensitivity of 95.7% (79.0-99.2%), specificity of 75% (30.1-95.4%), accuracy of 88.0% (67.7-100.0%) and odds ratio of 7.5 (1.16-48.63 [p=0.005]) for detection of GS ≥3+4. Likewise, if a sensitivity of > 90% for detection of GS ≥ 4+3 is wanted, e.g. to identify high risk PCa during uPAR image-based active surveillance then a cutoff of SUV_{max} = 3.725 could be applied (Figure 4). In discrimination of GS ≥ 4+3 vs. ≤ 3+4 the suggested cut-off results in a sensitivity of 92.9% (68.5-98.7%), specificity of 61.5% (35.5-82.3%), accuracy of 75.8% (56.7-95.0%) and odds ratio of 2.44 (1.08-5.53 [p=0.004]). Examples of SUV_{max} readout in two patients with GS 8 and 3+4, respectively, are shown in Figure 5.

Seventeen patients underwent radical prostatectomy, where three (17.6 %) were upgraded in GS compared to their biopsy results (two patients with GS 3+3 and one patient with GS 4+3), while two patients (11.7 %) were downgraded (one with GS 4+4 and one with GS 4+5). Applying the suggested SUVmax cut-off for discriminating GS ≥ 4+3 vs. ≤ 3+4 resulted in a sensitivity of 88.9% (51.8-99.7), specificity of 62.5% (24.5-91.5) and accuracy of 76.5% (50.1-93.2). As only one patient had

GS 3+3 in final histopathology, the suggested SUVmax cut-off for identifying GS ≥ 3+4 has not been tested in this subpopulation.

There was no significant correlation between SUV_{max} and PSA or between GS and PSA.

DISCUSSION

The main finding and primary outcome measure of this phase II clinical trial using the uPAR-targeted PET ligand ^{68}Ga-NOTA-AE105 in PCa patients was a correlation between uPAR-PET ligand uptake and GS obtained from biopsy material. This suggests that uPAR-PET potentially could serve a role as a substitute for, at least part of the invasive biopsies. An SUV_{max} cut-off could be established obtaining a high sensitivity for identifying patients with GS ≥ 3+4 from patients with GS ≤ 3+3 , which holds important prognostic information regarding adverse surgical pathology, risk of biochemical recurrence, metastasis and PCa specific mortality (*24*). Especially for patients in active surveillance, this method may be a valuable tool to non-invasively evaluate the need for repeated biopsies. Furthermore, addition of uPAR PET to mpMRI could be applied in biopsy guiding when indicated in order to target the lesions with the highest SUV_{max} and thereby highest uPAR expression.

It should be noted that uPAR PET readouts should be performed in the tumor why fusion with MRI or other tumor delineating imaging is needed. The tumoral ligand uptake, especially in low GS tumors is not sufficient for delineation of the tumor on PET images alone as the strength of uPAR-PET is the dynamic range leading to low uptake in low grade tumors. Also, and for the same reason, uPAR-PET is unlikely to be useful for metastatic staging where other modalities should be applied.

PET ligands targeted prostate-specific membrane antigen (PSMA) have also been investigated for non-invasive evaluation of GS. Some clinical studies of PSMA PET find a correlation between ^{68}Ga-PSMA-11 uptake and GS, mainly driven by high uptake in GS 9-10 (*25*–*27*). However, the published results show considerable overlap between all GS categories making meaningful cut-off values impossible to establish. Furthermore, a PET/MRI study with prostatectomy histopathology as reference found no correlation between ^{68}Ga-PSMA-11 uptake and GS (*28*). Although PSMA PET undoubtedly can play a major role in management of PCa patients, e.g. in staging, it cannot be considered as an appropriate method for GS estimation.

It could be speculated whether the correlation with GS obtained by uPAR-PET could have been obtained through mpMRI alone. Our study was not designed to answer this question and we cannot rule out that mpMRI in these patients would have correlated with GS. However, if so, we only see this as an advantage in particular if the combined information obtained from uPAR-PET and mpMRI could lead to even better correlation with GS. Therefore, in future large scale studies we plan a design that can compare the information obtained from uPAR-PET with that from mpMRI as well as study the added value of combining the two modalities and whether this leads to an even stronger correlation between imaging and GS.

As an exploratory, single center, phase II clinical trial the present study has inherited limitations. Due to the limited number of observations, the statistical analysis and diagnostic performance have broad confidence intervals. However, results from the present study will serve as an encouraging basis for designing future phase III clinical trials with larger number of patients. Further studies are needed before more firm conclusions can be drawn about the clinical utility and

potential of uPAR PET/mpMRI. Furthermore, when based on a much larger number of patients, the SUV_{max} cut-off values can be more firmly established and the added value of an integrated PET/mpMRI investigated.

Another issue to address is the selection of biopsies as reference for the PET/mpMRI results. Biopsies are prone to sampling error, documented by a relatively frequent up- or downgrading of GS in studies of prostatectomy specimens (*29*,*30*). Biopsies were chosen as primary reference, as the purpose of the study was to investigate if uPAR-PET could serve as a non-invasive alternative to the current biopsy regimen. Our study included patients with low-risk disease on active surveillance, which is a population of particular interest in the context of non-invasive risk stratification and where the utility of uPAR-PET may be highest. However, in these patients prostatectomy is not routinely performed and therefore biopsies are the only accessible samples for histological grading in all patients. Reducing the number of biopsies in active surveillance would be of significant value as biopsies are not only uncomfortable for the patient, but also hampered by side-effects such as bleeding and infection (*31*).

In our study population a subgroup did undergo prostatectomy and of these nearly 30 % had a different GS on final pathology compared to the previous biopsy. Although based on a limited number of patients, data from prostatectomies also supported our results regarding SUV cut-off for discrimination of GS ≥ 4+3 vs. ≤ 3+4.

Another limitation of the study is the selection of index lesions. We selected only to include lesions with a PI-RADS score of ≥ 4 in the study, in order to reduce the number of false

positives. As the majority of patients with PI-RADS 4-5 lesions have clinically significant PCa, it could be argued that the study population did not adequately represent patients with low-risk disease. However, a substantial part of the included patients in our study were candidates for active surveillance. Especially in these patients uPAR PET may aid to determine the need for close monitoring. A planned future study will be specifically aimed at patients in active surveillance and include lower grades of PI-RADS lesions.

As we used MRI-guided uPAR-PET, ideally the biopsies in the study cohort should also have been performed as MRI-targeted fusion biopsy (software-assisted MRI-transrectal ultrasound fusion or in-bore MRI target biopsy). However, at the time of inclusion of patients, equipment for software-assisted fusion or in-bore biopsy was not available at our facility, which prompted the application of MRI-directed cognitive registration. This method has been reported to yield lower detection rates of PCa compared to the other MRI-targeted techniques (*32*,*33*). However, we expect that such biopsies would most likely correlate even better with our uPAR-PET imaging biopsies.

In conclusion, this phase II clinical trial of uPAR PET/MRI using ^{68}Ga-NOTA-AE105 showed promising results for use in PCa patients. uPAR-PET ligand accumulation correlated with GS, which indicates that non-invasive evaluation of prostate cancer may potentially replace, at least in part, the biopsies in active surveillance. Based on the current data, a phase III study is planned to further study the utility in active surveillance. In addition, studies in various clinical settings of PCa are also planned to investigate the independent prognostic value of uPAR PET/MRI.

DISCLOSURES

AK and JM are inventors on a patent of the composition of matter of uPAR PET (WO 2014086364) and co-founders of Curasight, which has licensed the uPAR PET technology. No other potential conflicts of interest relevant to this article exist

ACKNOWLEDGEMENTS

This project received funding from the European Union's Horizon 2020 research and innovation programme under grant agreements no. 670261 (ERC Advanced Grant) and 668532 (Click-It), the Lundbeck Foundation, the Novo Nordisk Foundation, the Innovation Fund Denmark, the Danish Cancer Society, Arvid Nilsson Foundation, Svend Andersen Foundation, the Neye Foundation, the Research Foundation of Rigshospitalet, the Danish National Research Foundation (grant 126), the Research Council of the Capital Region of Denmark, the Danish Health Authority, the John and Birthe Meyer Foundation and Research Council for Independent Research.

KEY POINTS

QUESTION: Is there a correlation between uptake of the positron emission tomography (PET) ligand ^{68}Ga-NOTA-AE105 targeted urokinase-type plasminogen activator (uPAR) and Gleason Score in prostate cancer?

PERTINENT FINDINGS: A phase II clinical trial of uPAR PET/MRI in 27 patients with prostate cancer found standardized uptake value (SUV) in tumor had a significant positive correlation with Gleason Score obtained by biopsy. SUV thresholds could be established to discriminate between low- and intermediate risk Gleason Score.

IMPLICATIONS FOR PATIENT CARE: uPAR PET/MRI could be a promising method for non-invasive evaluation of PCa, which may in the future potentially reduce the need for repeated biopsies, e.g. in active surveillance.

REFERENCES

1. Tosoian JJ, Mamawala M, Epstein JI, et al. Intermediate and longer-term outcomes from a prospective active-surveillance program for favorable-risk prostate cancer. *J Clin Oncol*. 2015;33:3379-3385.

2. Thurtle D, Rossi SH, Berry B, Pharoah P, Gnanapragasam VJ. Models predicting survival to guide treatment decision-making in newly diagnosed primary non-metastatic prostate cancer: a systematic review. *BMJ Open*. 2019;9:e029149.

3. Gnanapragasam VJ, Bratt O, Muir K, et al. The Cambridge Prognostic Groups for improved prediction of disease mortality at diagnosis in primary non-metastatic prostate cancer: a validation study. *BMC Med*. 2018;16:31.

4. Mottet N, van den Bergh RCN, Briers E, et al. EAU Prostate cancer guidelines. Edn. presented at the EAU Annual Congress Barcelona 2019. https://uroweb.org/guideline/prostate-cancer/. Accessed June 12, 2019.

5. Drost F-JH, Osses DF, Nieboer D, et al. Prostate MRI, with or without MRI-targeted biopsy, and systematic biopsy for detecting prostate cancer. *Cochrane Database Syst Rev*. 2019;4:CD012663.

6. Ahmed HU, El-Shater Bosaily A, Brown LC, et al. Diagnostic accuracy of multi-parametric MRI and TRUS biopsy in prostate cancer (PROMIS): a paired validating confirmatory study. *Lancet (London, England)*. 2017;389:815-822.

7. Sonn GA, Fan RE, Ghanouni P, et al. Prostate magnetic resonance imaging interpretation varies substantially across radiologists. *Eur Urol Focus*. 2019;5:592-599.

8. Huang Z, Wang L, Wang Y, et al. Overexpression of CD147 contributes to the chemoresistance of head and neck squamous cell carcinoma cells. *J Oral Pathol Med*. 2013;42:541-546.

9. Wang K, Xing Z-H, Jiang Q-W, et al. Targeting uPAR by CRISPR/Cas9 system attenuates cancer malignancy and multidrug resistance. *Front Oncol*. 2019;9:80.

10. Eastman BM, Jo M, Webb DL, Takimoto S, Gonias SL. A transformation in the mechanism by which the urokinase receptor signals provides a selection advantage for estrogen receptor-expressing breast cancer cells in the absence of estrogen. *Cell Signal*. 2012;24:1847-1855.

11. Rabbani SA, Ateeq B, Arakelian A, et al. An anti-urokinase plasminogen activator receptor antibody (ATN-658) blocks prostate cancer invasion, migration, growth, and experimental skeletal metastasis in vitro and in vivo. *Neoplasia*. 2010;12:778-788.

12. Mahmood N, Mihalcioiu C, Rabbani SA. Multifaceted role of the urokinase-type plasminogen activator (uPA) and its receptor (uPAR): Diagnostic, prognostic, and therapeutic applications. *Front Oncol*. 2018;8:24.

13. Kumano M, Miyake H, Muramaki M, Furukawa J, Takenaka A, Fujisawa M. Expression of urokinase-type plasminogen activator system in prostate cancer: correlation with clinicopathological outcomes in patients undergoing radical prostatectomy. *Urol Oncol*. 2009;27:180-186.

14. Cozzi PJ, Wang J, Delprado W, et al. Evaluation of urokinase plasminogen activator and its receptor in different grades of human prostate cancer. *Hum Pathol*. 2006;37:1442-1451.

15. Persson M, Madsen J, Østergaard S, et al. Quantitative PET of human urokinase-type plasminogen activator receptor with 64Cu-DOTA-AE105: implications for visualizing cancer invasion. *J Nucl Med*. 2012;53:138-145.

16. Persson M, Hosseini M, Madsen J, et al. Improved PET imaging of uPAR expression using new (64)Cu-labeled cross-bridged peptide ligands: comparative in vitro and in vivo studies. *Theranostics*. 2013;3:618-632.

17. Persson M, Liu H, Madsen J, Cheng Z, Kjaer A. First (18)F-labeled ligand for PET imaging of uPAR: in vivo studies in human prostate cancer xenografts. *Nucl Med Biol*. 2013;40:618-624.

18. Persson M, El Ali HH, Binderup T, et al. Dosimetry of 64Cu-DOTA-AE105, a PET tracer for uPAR imaging. *Nucl Med Biol*. 2014;41:290-295.

19. Persson M, Kjaer A. Urokinase-type plasminogen activator receptor (uPAR) as a promising new imaging target: potential clinical applications. *Clin Physiol Funct Imaging*. 2013;33:329-37.

20. Persson M, Skovgaard D, Brandt-Larsen M, et al. First-in-human uPAR PET: Imaging of Cancer Aggressiveness. *Theranostics*. 2015;5:1303-1316.

21. Skovgaard D, Persson M, Brandt-Larsen M, et al. Safety, dosimetry, and tumor detection ability of 68Ga-NOTA-AE105: First-in-human study of a novel radioligand for uPAR PET imaging. *J Nucl Med*. 2017;58:379-386.

22. Vargas HA, Hötker AM, Goldman DA, et al. Updated prostate imaging reporting and data system (PIRADS v2) recommendations for the detection of clinically significant prostate cancer using multiparametric MRI: critical evaluation using whole-mount pathology as standard of reference. *Eur Radiol*. 2016;26:1606-1612.

23. Budczies J, Klauschen F, Sinn BV., et al. Cutoff Finder: A comprehensive and straightforward web application enabling rapid biomarker cutoff optimization. *PLoS One*. 2012;7:e51862.

24. Kane CJ, Eggener SE, Shindel AW, Andriole GL. Variability in outcomes for patients with intermediate-risk prostate cancer (Gleason Score 7, International Society of Urological Pathology Gleason group 2-3) and implications for risk stratification: A systematic review. *Eur Urol Focus*. 2017;3:487-497.

25. Uprimny C, Kroiss AS, Decristoforo C, et al. (68)Ga-PSMA-11 PET/CT in primary staging of prostate cancer: PSA and Gleason score predict the intensity of tracer accumulation in the primary tumour. *Eur J Nucl Med Mol Imaging*. 2017;44:941-949.

26. Sathekge M, Lengana T, Maes A, et al. 68Ga-PSMA-11 PET/CT in primary staging of prostate carcinoma: preliminary results on differences between black and white South-Africans. *Eur J Nucl Med Mol Imaging*. 2018;45:226-234.

27. Hicks RM, Simko JP, Westphalen AC, et al. Diagnostic Accuracy of (68Ga)-PSMA-11 PET/MRI compared with multiparametric MRI in the detection of prostate cancer. *Radiology*. 2018;289:730-737.

28. Eiber M, Weirich G, Holzapfel K, et al. Simultaneous 68Ga-PSMA HBED-CC PET/MRI improves the localization of primary prostate cancer. *Eur Urol*. 2016;70:829-836.

29. Epstein JI, Feng Z, Trock BJ, Pierorazio PM. Upgrading and downgrading of prostate cancer from biopsy to radical prostatectomy: Incidence and predictive factors using the modified Gleason grading system and factoring in tertiary grades. *Eur Urol*. 2012;61:1019-1024.

30. Treurniet KM, Trudel D, Sykes J, Evans AJ, Finelli A, Van der Kwast TH. Downgrading of biopsy based Gleason score in prostatectomy specimens. *J Clin Pathol*. 2014;67:313-318.

31. Loeb S, Carter HB, Berndt SI, Ricker W, Schaeffer EM. Complications after prostate biopsy: Data from SEER-Medicare. *J Urol*. 2011;186:1830-1834.

32. Wegelin O, van Melick HHE, Hooft L, et al. Comparing three different techniques for magnetic resonance imaging-targeted prostate biopsies: A systematic review of in-bore versus magnetic resonance imaging-transrectal ultrasound fusion versus cognitive registration. Is there a preferred technique? *Eur Urol*. 2017;71:517-531.

33. Stabile A, Dell'Oglio P, Gandaglia G, et al. Not all multiparametric magnetic resonance imaging–targeted biopsies are equal: The impact of the type of approach and operator expertise on the detection of clinically significant prostate cancer. *Eur Urol Oncol*. 2018;1:120-128.

Tables

Patients, N = 27	
Age (years), mean (range)	66.6 (50.2-79.9)
PSA (ng/ml), mean (range)	28.8 (7.0-56.0)
Clinical tumor stage, n (%)	
cT1	9 (33.3 %)
cT2	9 (33.3 %)
cT3	9 (33.3 %)
Gleason score, n (%)	
3+3	4 (14.8 %)
3+4	9 (33.3 %)
4+3	5 (18.5 %)
8 (4+4/3+5/5+3)	2 (7.4 %)
9 (4+5/5+4)	7 (25.9 %)
PI-RADS score, n (%)	
4	10 (37.0%)
5	17 (63.0 %)

Table 1: Patient characteristics

	N	Reader 1 Mean SUVmax (SEM)	Reader 2 Mean SUVmax (SEM)	Mean SUVmax (SEM)
GS 3+3	4	2.48 (0.54)	2.83 (0.53)	2.65 (0.51)
GS 3+4	9	4.13 (0.46)	3.82 (0.38)	3.98 (0.41)
GS 4+3	5	4.80 (0.91)	3.98 (0.22)	4.39 (0.56)
GS 8	2	4.65 (0.25)	4.65 (0.25)	4.65 (0.25)
GS 9	7	5.22 (0.49)	4.86 (0.41)	5.04 (0.43)

Table 2. SUVmax values of Gleason score (GS) subgroups reported as mean and standard error of the mean (SEM).

Figures and legends:

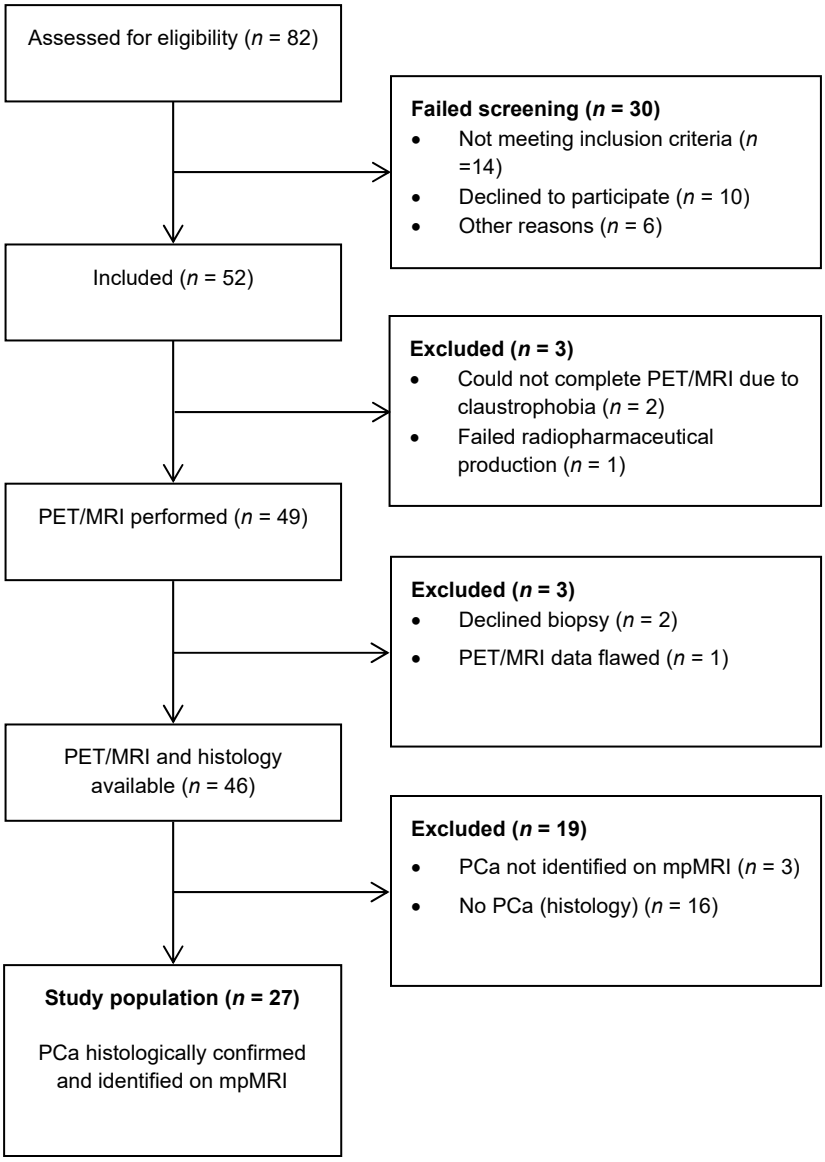

Figure 1: Consort flow diagram of inclusion process

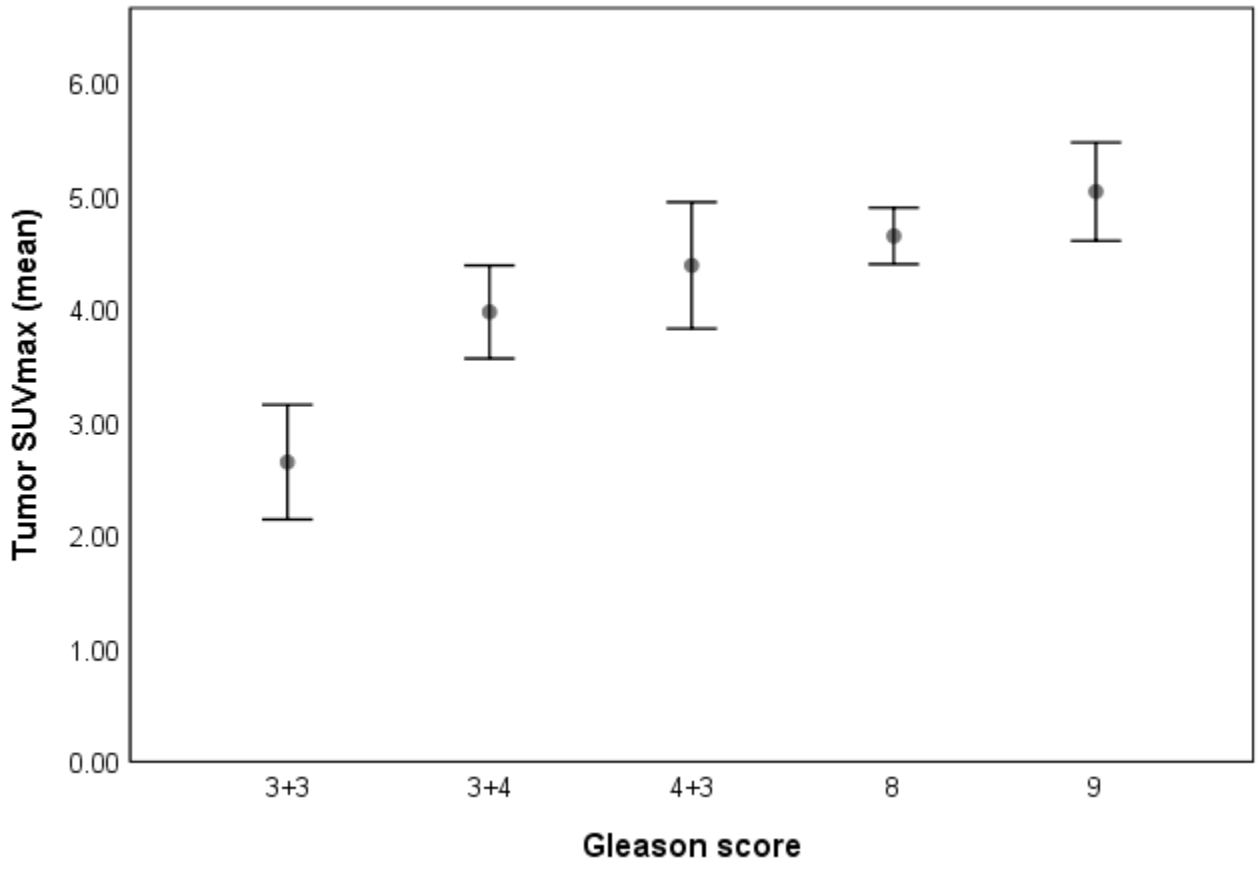

Figure 2: Relation between uPAR-PET SUVmax and Gleason score. Values are mean +/- SEM.

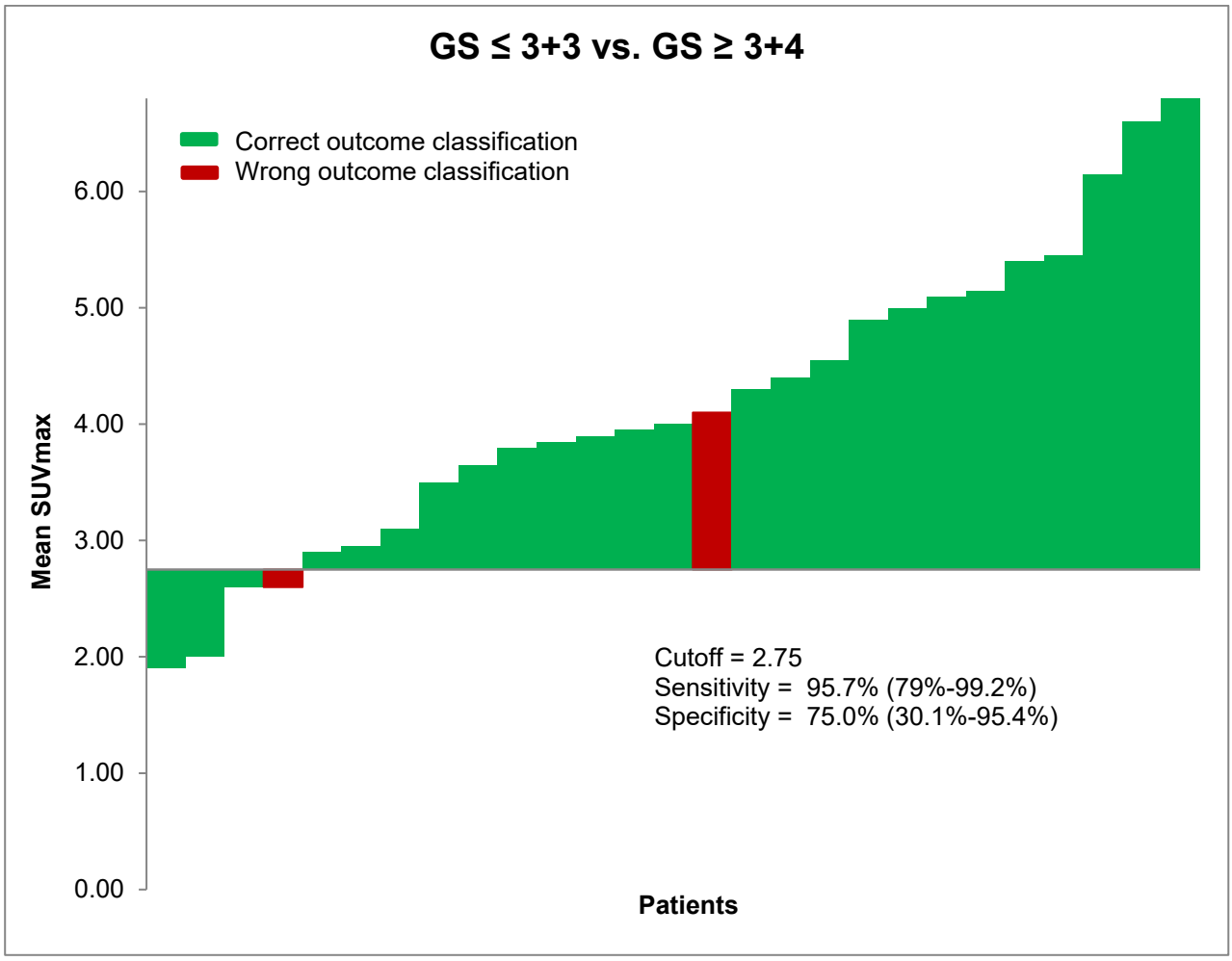

Figure 3: Waterfall plot of SUVmax in tumor for discrimination of GS ≤ 3+3 vs. GS ≥ 3+4

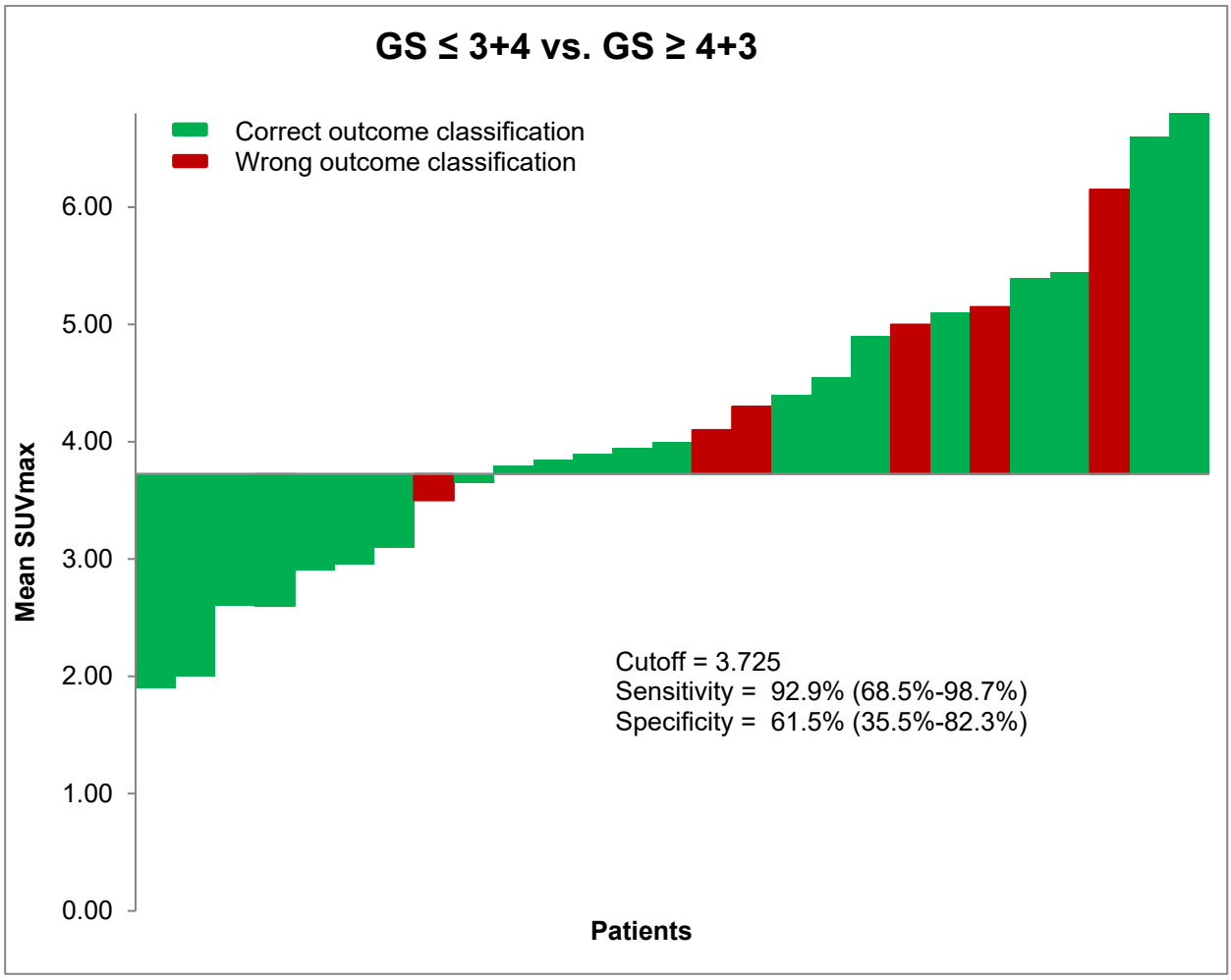

Figure 4: Waterfall plot of SUVmax in tumor for discrimination of GS ≤ 3+4 vs. GS ≥ 4+3

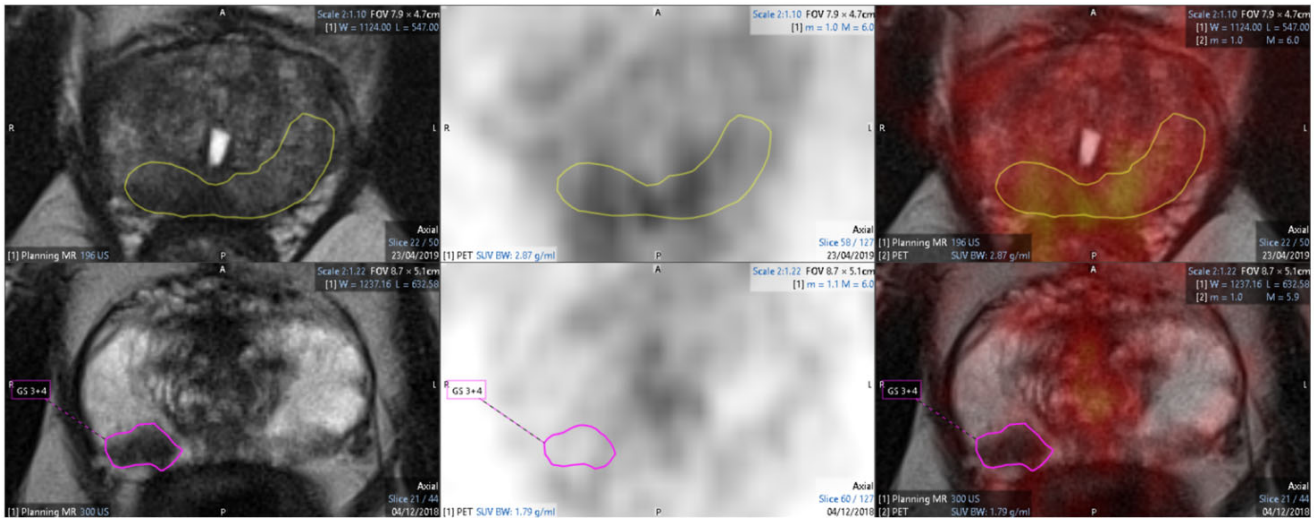

Figure 5: Delineated tumor VOIs in uPAR PET/MRI (transaxial T2w image) of a patient with Gleason score 8 prostate cancer (upper panel; SUVmax = 4.6) and a patient with Gleason score 3+4 (lower panel; SUVmax=2.8).